Nuclear Science and Techniques (2022) 33:151
https://doi.org/10.1007/s41365-022-01147-2

Analysis on the influencing factors of radioactive tritium leakage and diffusion from an indoor high-pressure storage vessel

Chang-Jun Li[1,2] · Xing-Fu Cai[1] · Ming-Qing Xiao[2] · Yong-Gang Huo[1] · Peng Xu[1] · Su-Fen Li[1] · Xiao-Yan Cao[1]

Received: 24 August 2022 / Revised: 12 October 2022 / Accepted: 17 October 2022 / Published online: 6 December 2022

Abstract

Radioactive tritium leakage from high-pressure storage vessels is a common nuclear leakage event. Different leakage conditions have different effects on tritium diffusion, resulting in different degrees of radioactive hazards. This study focuses on tritium leakage from high-pressure storage vessels and analyzes the influence of different leakage orifice shapes, leakage positions, and the presence of obstacles in the scene space on tritium leakage diffusion. The results show that there is little difference in the radial diffusion velocity of tritium gas along the jet axis between circular and square leakage orifices. The radial diffusion velocity of tritium gas in the long-axis direction of the rectangular leakage orifice is larger than that in the short-axis direction, and the larger the aspect ratio of the rectangle is, the greater the difference is in the diffusion velocity. In addition, leakage from the storage vessel below the air inlet is beneficial to the dilution of tritium, whereas leakage from the air vents leads to a slow decrease in the tritium concentration. The obstacles present in the tritium scene space hinder the migration of tritium gas and prolong the time for the tritium concentration to reach stabilization. This study provides a theoretical basis for the disposal of tritium in tritium leakage accidents by analyzing the influence of different leakage conditions in storage vessels on tritium gas diffusion.

Keywords Tritium leakage · Leakage orifice shape · Leakage position · Obstacles

1 Introduction

Radioactive tritium is one of the raw materials used in nuclear fusion reactions and poses a radioactive hazard when leakage occurs because of the release of β-rays into the environment [1]. Consequently, tritium is usually stored in high-pressure vessels that can reach pressures of up to hundreds of atmospheres. A radioactive environment is formed by a tritium leakage when the storage vessel is accidentally damaged by external effects. However, different leakage conditions, including the leakage orifice shapes, leakage positions, and the existence of obstacles in the scene space of the leakage, have different effects on the migration and mixing behaviors of tritium gas. This will affect the decision-making involved in the emergency treatment of tritium leakage. Therefore, research on the factors influencing tritium leakage and diffusion from high-pressure vessels has practical significance.

Presently, nuclear leakage accidents in nuclear power plant reactors have received the greatest focus in this area. For example, Zhao et al. [2] simulated the diffusion of radionuclides from a marine nuclear reactor in an enclosed environment during a nuclear leakage accident. Esfandiari et al. [3] proposed a method integrating deterministic events and probabilistic assessment to analyze the risk of accidents at nuclear power plants, with the results indicating that the method can effectively assess the frequency and overall risk of accidents. Deng et al. [4] monitored nuclear reactors for leakage by following changes in tritium concentration in the environment. Wang B E et al. [5] used the computational fluid dynamics (CFD) code FLUENT to establish a CFD discrete phase model, through which supersonic jet flow and dust transport induced by air ingress in a fusion reactor were analyzed. This provided a basis for nuclear safety analysis

This work was supported by the Youth Innovation Team of Shaanxi Universities and the Pre-research Fund (No. 50926050408).

✉ Xing-Fu Cai
17791477740@sina.cn

[1] Xi'an Research Institute of High-Tech, Xi'an 710025, China

[2] Air Force Engineering University, Xi'an 710051, China

and accident prevention for future fusion reactors. Barzegari et al. [6] evaluated the damage to fuel rods after a severe accident in the Bushehr pressurized water reactor power plant and used the MELCOR code to calculate the shortest available time for accident prevention. Gu et al. [7] developed a multi-physics coupled code MPC-LBE, based on a CFD framework and verified by a mature simulation code, to analyze the safety of an LBE-cooled reactor. Research on tritium leakage accidents has been conducted mainly from two perspectives—intentional tritium release experiments and numerical simulations of tritium leakage of nuclear fusion reactors. For the tritium release experiments, the Los Alamos National Laboratory (LANL) of the United States has built a Tritium Systems Test Assembly (TSTA) [8–11] and conducted tritium release experiments. Meanwhile, they have also developed a series of simulation models of tritium diffusion, such as FLOW-3D and GASFLOW II. Furthermore, the Japan Atomic Energy Research Institute (JAERI) has also built a tritium release device, Caisson Assembly for Tritium Safety (CATS) [12–15], which could obtain more accurate tritium release experimental data with a smaller volume than TSTA could. They improved upon the accuracy of the LANL tritium simulation code. Nevertheless, the ventilation settings in these experiments were alike, and the factors affecting the detritiation efficiency were hardly modified. With regard to the numerical simulation of tritium leakage, a large number of simulation studies modeling tritium behavior have been conducted both in China and abroad. Li et al. [16] numerically simulated the tritium diffusion in a low-pressure tritium leakage accident from a storage vessel under open and closed spatial conditions. Liu [17] studied the effect of ventilation on tritium concentration and diffusion in a tritium leakage accident in a Test Blanket Module (TBM) glove box but with few ventilation scenarios. Wei [18] simulated the tritium migration and detritiation behavior during accidents in tritium factory rooms and analyzed the effects of ventilation design, temperature conditions, and wall materials on detritiation. Li et al. [19, 20] examined methods for optimizing ventilation conditions for tritium leakage in a high-pressure and developed a ventilation method with relatively high detritiation efficiency.

In summary, much research has been conducted involving the simulation of tritium migration and mixing behavior during tritium leakage accidents throughout the world, and the detritiation efficiency has been improved by the optimization of the air vent design. However, there remains a dearth of research on the effects of different leakage conditions on the diffusion of tritium gas. Regarding the tritium leakage issue in high-pressure storage vessels, this study investigates the influence of different leakage orifice shapes, leakage positions, and the existence of obstacles in the scene space on tritium leakage and diffusion via FLUENT software and verifies the accuracy of the model through comparison with CATS test data.

2 Tritium leakage and diffusion theory

In this study, a high-pressure storage vessel with pressures of hundreds of atmospheres is examined. When a high-pressure storage vessel has a small orifice leakage, the tritium behavior deviates from an ideal gas. Because tritium molecules are compressed in a high-pressure environment, the compressibility factor is larger than 1. Therefore, the traditional ideal gas model is not accurate for describing the tritium leakage behavior in a high-pressure storage vessel. The Abel–Noble equation of state [21] (AN-EOS), which corrects the specific volume of tritium molecules, provides an accurate description of high-pressure tritium leakage, and the relationship between the pressure in the and the correction term is obtained as follows:

$$p(v-b)=R_{\mathrm{g}}T, \tag{1}$$

where p is the pressure, v is the specific volume, b is the correction term of the gas molecule and $b=7.691\times10^{-3}$ $\mathrm{m^3\cdot kg^{-1}}$, R_{g} is the gas constant, and T is the temperature.

Assuming that the gas leakage process is isentropic, it can be obtained from the AN-EOS equation [22],

$$p(v-b)^n=\text{constant}, \tag{2}$$

where n is the specific heat capacity ratio.

For a fixed-volume storage vessel, the velocity of leakage is closely related to the pressure inside the. When the ratio of the pressure inside the to the ambient pressure is greater than the critical pressure ratio v_{cr}, the airflow velocity at the leakage orifice reaches the local speed of sound, that is,

$$c_{\mathrm{f}}=\frac{v_2}{v_2-b}\sqrt{nR_{\mathrm{g}}T_2}=v_2\sqrt{n\frac{p_2}{v_2-b}}, \tag{3}$$

where

$$v_{\mathrm{cr}}=\frac{p_2}{p_i}=\left(1+\frac{n-1}{2}\left(\frac{v_2}{v_2-b}\right)^2\right)^{\frac{n}{1-n}}.$$

However, when the ratio of the pressure inside the to the ambient pressure is less than or equal to the critical pressure ratio v_{cr}, subsonic flow occurs at the leakage orifice. The pressure at the leakage orifice decreases to the ambient pressure, that is, $p_2=p_{\mathrm{amb}}$, and remains unchanged thereafter. The tritium leakage velocity is

$$c_f = \sqrt{\frac{2n}{n-1} p_i (v_i - b)\left(1 - \left(\frac{p_2}{p_i}\right)^{\frac{n-1}{n}}\right)}, \quad (4)$$

where p_{amb} is the ambient pressure, v_{cr} is the critical pressure ratio, c_f is the tritium leakage velocity, v_2 is the specific volume at the leakage orifice, T_2 is the temperature at the leakage orifice, p_2 is the pressure at the leakage orifice, and p_i is the pressure inside the storage vessel.

Given a pressure of up to hundreds of atmospheres in the storage vessel, when the vessel is broken and tritium leakage occurs, the initial velocity of the tritium gas is relatively high, and jet flow and diffusion simultaneously exist in the closed space. Therefore, the realizable k–ε model [23], suitable for complex flow types, was employed, with the transport equations for k and ε described as follows:

$$\frac{\partial(\rho k)}{\partial t} + \frac{\partial(\rho k u_i)}{\partial x_i} = \frac{\partial}{\partial x_j}\left[\left(\mu + \frac{\mu_t}{\sigma_k}\right)\frac{\partial k}{\partial x_j}\right] + G_k - \rho\varepsilon, \quad (5)$$

$$\frac{\partial(\rho\varepsilon)}{\partial t} + \frac{\partial(\rho\varepsilon u_i)}{\partial x_i} = \frac{\partial}{\partial x_j}\left[\left(\mu + \frac{\mu_t}{\sigma_\varepsilon}\right)\frac{\partial \varepsilon}{\partial x_j}\right] + \rho C_1 S_\varepsilon - C_2\rho\frac{\varepsilon^2}{k+\sqrt{u\varepsilon}}. \quad (6)$$

Here,

$$C_1 = \max\left(0.43, \frac{\eta}{\eta+5}\right),$$

$$\mu_t = \rho C_\mu \frac{k^2}{\varepsilon},$$

where k is the turbulent kinetic energy; ε is the rate of dissipation; ρ is the density of the gas mixture, kg/m^3; μ is the fluid dynamic viscosity; μ_t is the turbulent viscosity; σ_k is the Prandtl number of the turbulent kinetic energy k, $\sigma_k = 1.0$; σ_ε is the Prandtl number of the dissipation rate ε, $\sigma_\varepsilon = 1.2$; G_k is the generation term of the turbulent kinetic energy k caused by the average velocity gradient; S_ε is the source term of the dissipation rate; η is an effectiveness factor; C_2 is an empirical constant, $C_2 = 1.9$; C_μ is the calculation coefficient for the turbulent viscosity; $\boldsymbol{u}$ is the velocity vector.

3 Numerical simulation of tritium leakage

3.1 Scene construction and boundary

In this study, tritium leakage occurred in a space with two detritiation vents. The storage vessel was placed on the ground at the center of the scene; the vessel contained a tritium pressure of 34.5 MPa and a temperature of 300 K. Figure 1 shows the physical model of the tritium leakage. To accurately describe the variation in tritium concentration at $z = 1.5$ m in space, the average breathing height of

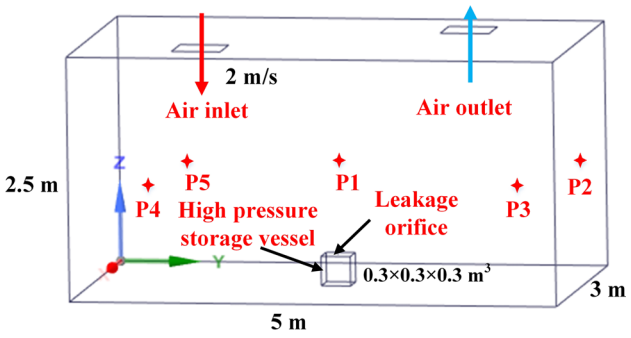

Fig. 1 Physical model

Table 1 Monitor point coordinates

Point	P1	P2	P3	P4	P5
x (m)	1.5	0.5	2.0	2.0	0.5
y (m)	2.5	4.5	4.5	0.5	0.5
z (m)	1.5	1.5	1.5	1.5	1.5

the operators, five monitoring points from P1 to P5 were set in the space. The coordinates of each monitoring point are listed in Table 1.

The boundary conditions of the leakage orifice were described by the AN-EOS model using user-defined functions, such as mass flow rate, pressure, and temperature. For the material setting, tritium gas [24] was added. The tritium gas had a molar mass of 6.034 kg kmol^{-1}, diffusion coefficient in air of 7.41×10^{-6} m^2 s^{-1}, specific heat capacity of 7243 J kg^{-1} K^{-1}, thermal conductivity of 0.1381 W m^{-1} K^{-1}, and viscosity coefficient of 1.259×10^{-5} kg m^{-1} s^{-1}. The wall material of the closed space was calcium carbonate, and the storage vessel was made of steel.

3.2 Different leakage conditions

Different leakage conditions have different effects on tritium diffusion. In this study, simulation calculations were performed considering different leakage orifice shapes, different leakage positions, and the existence of obstacles in the scene space. Specifically, the tested shapes of the leakage orifice were as follows: a 10 mm diameter circle, an 8.86 mm × 8.86 mm square, a 4 mm × 19.6 mm rectangle (rectangle 1) with an aspect ratio of 5, and a 2 mm × 39.3 mm rectangle (rectangle 2) with an aspect ratio of 18. Notably, the four leakage orifice shapes have the same leakage area. The three leakage positions were below the air inlet, far away from the vent, and below the air outlet. The obstacles used were one operator and one rectangular cube. Figure 2 shows the different leakage conditions. When examining the effects of the different leakage positions, the shape of the leakage orifice was uniformly simplified as a circle for the control

variables. The operator and box were located 0.5 m from the storage vessels on the left and right sides, respectively. Table 2 lists the obstacle dimensions.

4 Results and discussion

4.1 "Caisson" simulation verification

The tritium diffusion model is verified by comparing it with the experimental data from "CTAS" of JAERI [12]. First, the same conditions as the "CATS" experiment are set. Then, the calculated and experimentally determined tritium concentrations are compared. The tritium concentration can be monitored by TM1–TM4, the "Caisson" model, and the results are shown in Fig. 3.

Figure 3 shows a comparison of the tritium concentration at the monitoring points obtained by the simulation and "Caisson" experiment. The results reveal that the tritium concentration at TM2, which was the point closest to the release point in the simulation results, increased rapidly in the early stages of tritium release. The concentration at TM1 just above the release point peaked at approximately 40 s, and the concentration at TM3, farthest from the release point, tended to be stable after 160 s. The stable value of the tritium concentration in both the simulation and experimental results was approximately 1.5×10^{7} Bq m^{-3}. In short, in the simulation results, there were significant fluctuations in the tritium concentration at each monitoring point before the concentration stabilized. The main reasons are as follows. First, the time lag of the tritium gas flowing into the "Caisson" device after release in the experiment was not considered in the simulation. Second, the small amount of tritium gas released can lead to certain errors in the simulation. However, the stabilized tritium concentration was consistent with the experimental results, indicating that the model can be used to simulate the tritium release behavior.

Table 2 Obstacle dimensions

Name	Dimensions (mm^3)
Operator head	50×50×80
Operator body	300×200×400
Operator legs	50×50×800
Rectangular cube	800×500×1000

4.2 Different leakage shapes

When tritium gas leaks through small apertures from high-pressure storage vessels, the speed of leakage can reach the speed of sound. Different leak orifice shapes have diverse effects on the radial diffusion of the tritium gas. To thoroughly analyze the influence of the orifice shape on the tritium leakage and diffusion laws, numerical simulations were performed with circular, square, and rectangular leakage orifices. Cloud diagrams for the tritium gas jet flow and the variations in the tritium concentration along the jet axis were obtained with different leakage orifice shapes at $t=0.3$ s and $t=2$ s, as shown in Fig. 4.

Figure 4a–d shows the distribution of the mass fraction of tritium gas after 0.3 s of leakage at the circular, square, and

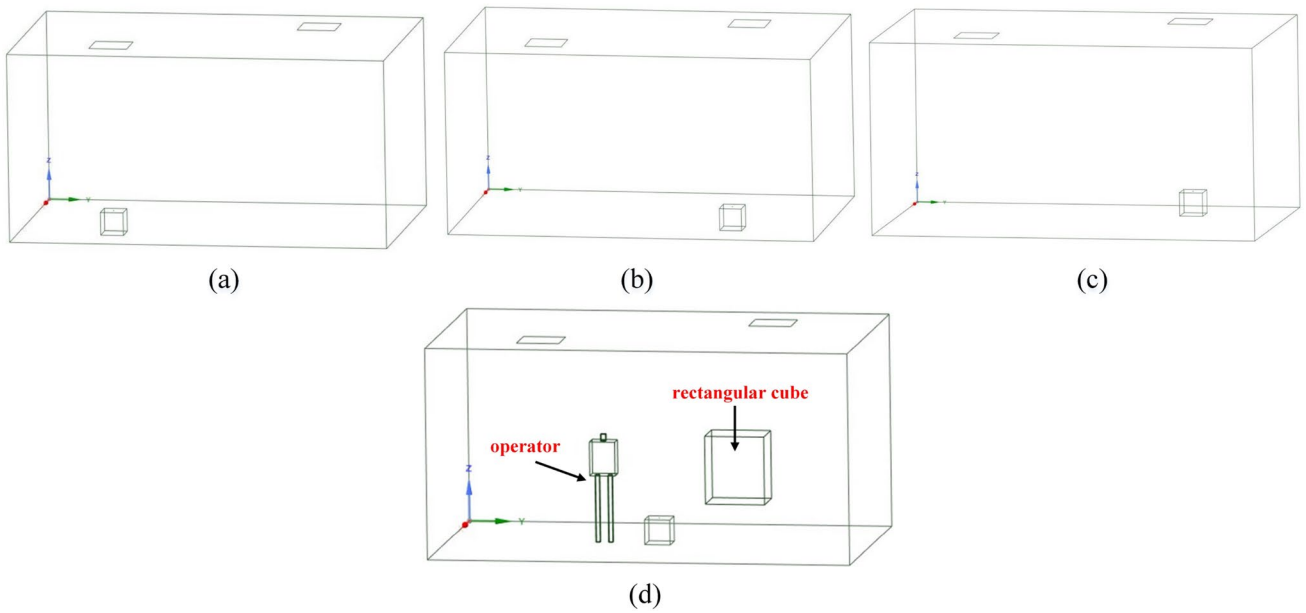

Fig. 2 (Color online) Different leakage conditions. a Below air inlet; b away from the vent; c below air outlet; **d** obstacles in the space

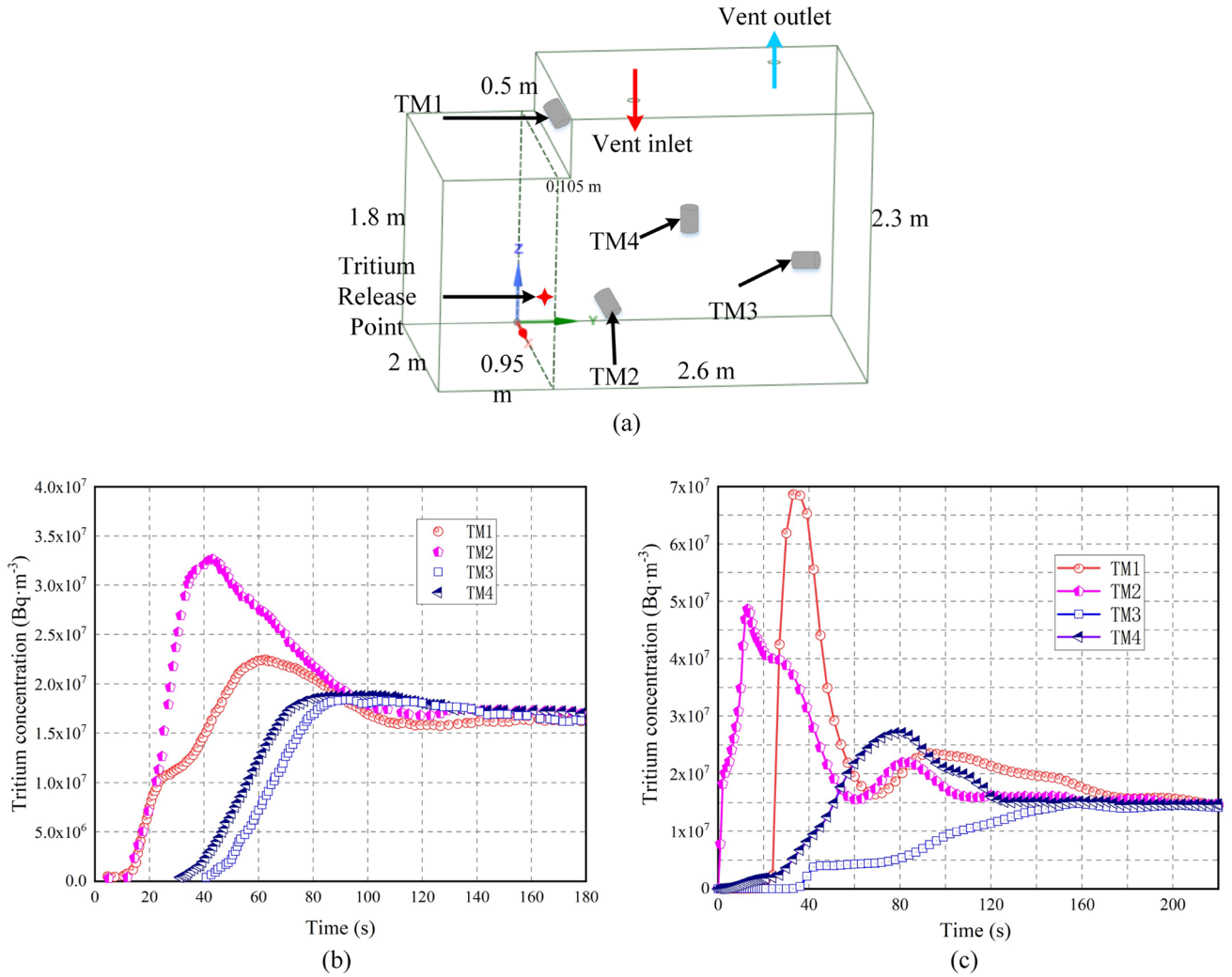

Fig. 3 (Color online) "Caisson" simulation verification. **a** Caisson geometric model; **b** experimental results; **c** simulation results

two rectangular leakage orifices, respectively. The results show that the tritium gas formed a strong jet in the leakage orifice plane during the early stages of the leakage, and the tritium gas jet was distributed evenly in the *YZ* plane and *XZ* plane of the circular and square leakage orifices, as shown in Fig. 4a, b, respectively, indicating that the radial diffusion velocity of tritium gas is relatively uniform under circular and square leakage orifices. The jet distribution for the rectangular leakage orifices showed an axis conversion phenomenon—the diffusion width of the tritium jet in the *YZ* plane (long-axis plane of the leakage orifice) narrowed, while that in the *XZ* plane (short-axis plane of the leakage orifice) widened. This axis conversion phenomenon became more evident with the increased aspect ratio of the rectangle, as shown in Fig. 4c, d. This implies a higher radial diffusion velocity and a narrowing jet width for the tritium gas in the long-axis plane of the rectangular leakage orifice, contrasting with a lower radial diffusion velocity and widening jet width in the short-axis plane. Hence, it is clear that a highly under-expanded gas forms a strong jet along the axis at the leakage orifice when high-pressure tritium gas leaks through small holes. The radial diffusion velocity of the tritium gas differs for different leakage orifice shapes. Specifically, the radial diffusion velocity is uniform at symmetrical leakage orifices, whereby the long-axis direction of the rectangular leakage orifice is conducive to the radial diffusion of tritium gas, while the short-axis direction hinders its radial diffusion. The difference in the radial diffusion velocity of tritium gas increases with the increase in the aspect ratio of the rectangular leakage orifice.

Figure 4e–h shows the distribution of mass fraction of tritium gas at different leakage orifices after 2 s of leakage. The results show that the tritium pressure in the vessels gradually decreases as the leakage continues, the axial jet width at the leakage orifices gradually narrows, and the jet width tends to be the same between the long-axis plane

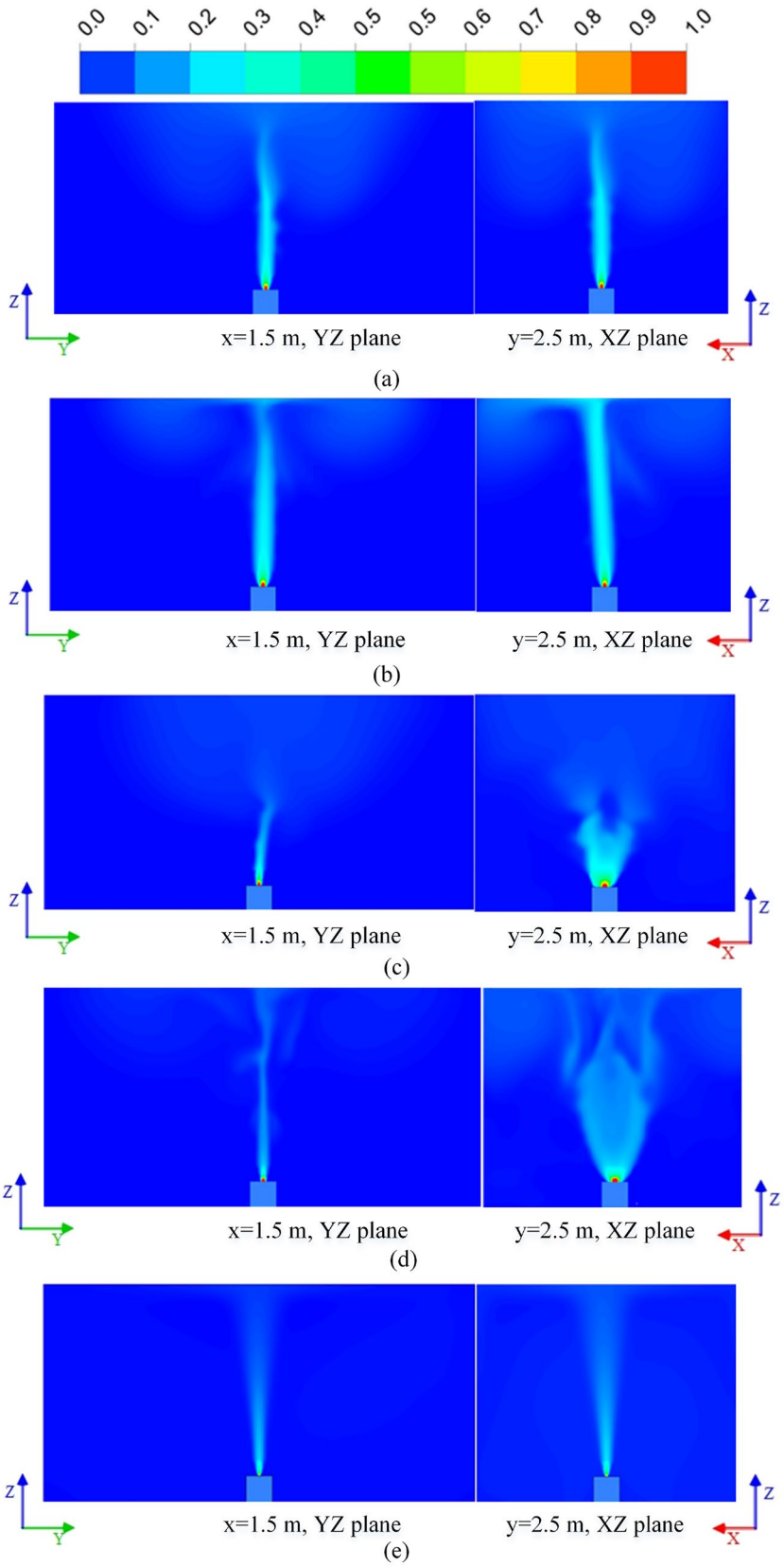

Fig. 4 (Color online) Different leakage shapes results. **a** Mass fraction of tritium gas at the circular leakage orifice at $t=0.3$ s; **b** mass fraction of tritium gas at the square leakage orifice at $t=0.3$ s; **c** mass fraction of tritium gas at rectangular leakage orifice 1 at $t=0.3$; **d** mass fraction of tritium gas at rectangular leakage orifice 2 at $t=0.3$ s; **e** mass fraction of tritium gas at the circular leakage orifice at $t=2$ s; **f** mass fraction of tritium gas at the square leakage orifice at $t=2$ s; **g** mass fraction of tritium gas at rectangular leakage orifice 1 at $t=2$ s; **h** mass fraction of tritium gas at rectangular leakage orifice 2 at $t=2$ s; **i** variations in tritium concentration along the jet axis

Fig. 4 (continued)

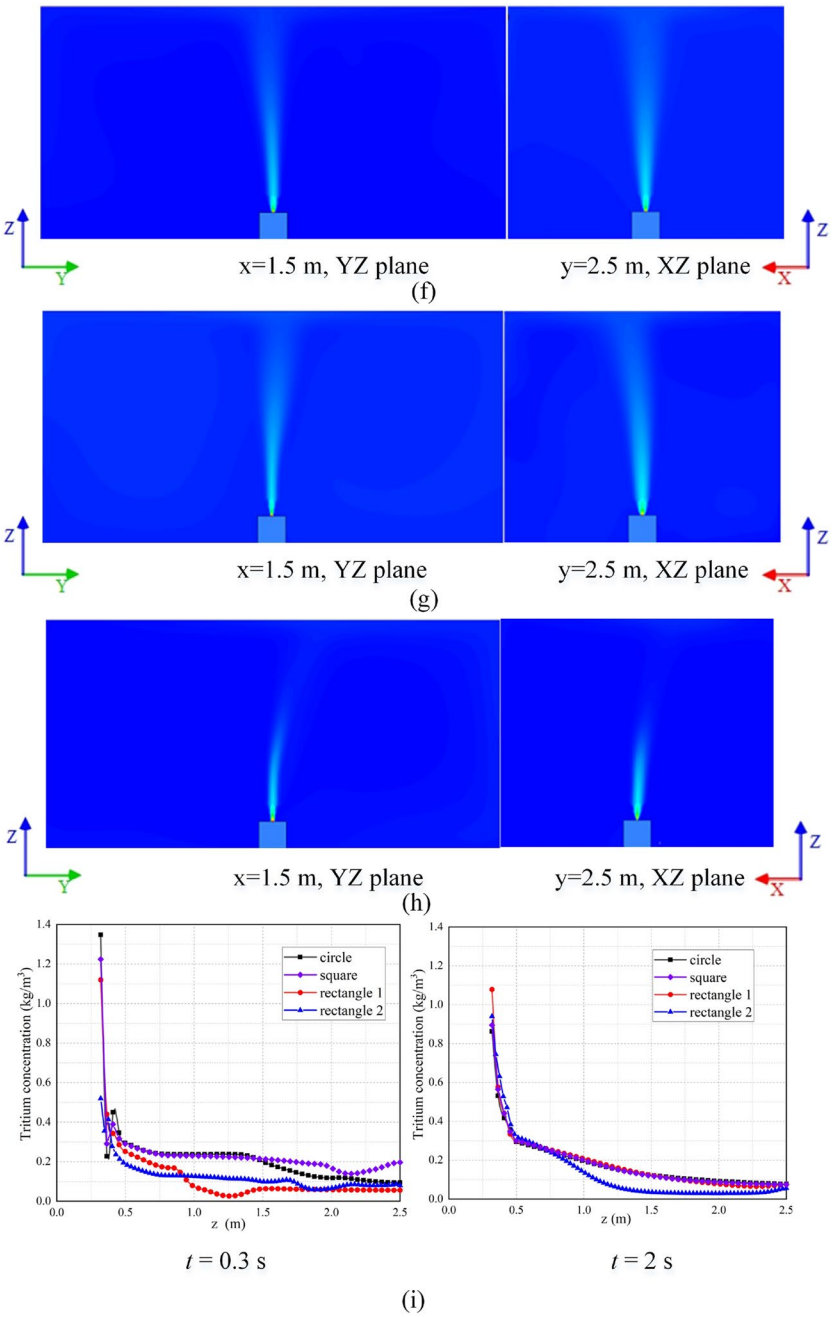

and the short-axis plane of the rectangular leakage orifices. Particularly, the jet length and width at rectangular leakage orifice 2 becomes significantly smaller. The difference in the radial diffusion velocity at different leakage orifices is small during the low-pressure tritium leakage, and the radial diffusion velocity of tritium gas increases with the rise in the aspect ratio of the rectangular leakage orifice.

Figure 4i displays the variation of tritium concentration along the jet axis at different leakage times. The results demonstrate that the closer the jet axis is to the leakage orifice, the higher the tritium concentration, whereas farther distances from the leakage orifice correspond to lower tritium concentrations. In the initial stage of the tritium leakage, namely at $t = 0.3$ s, the tritium concentration along the jet axis of the rectangular leakage orifice was smaller than that of the circular and square leakage orifices. This shows that the radial diffusion velocity of the tritium gas at the rectangular orifice is higher than that at the circular and square orifices, resulting in a lower tritium concentration along the axis. At $t = 2$ s, the variation of the tritium concentration along the jet axis at the circular, square, and rectangular 1 leakage orifices was the same; however, the tritium concentration was lower when the distance z between the jet axis and rectangular leakage orifice 2 was larger than 0.75 m.

This demonstrates that the circular, square, and rectangular 1 leakage orifices manifest little difference in the radial diffusion velocity of the tritium gas when the tritium pressure decreases. However, rectangular leakage orifice 2 is featured a relatively high radial diffusion velocity of tritium gas and low tritium concentration on the axis.

4.3 Different leakage positions

Tritium leakage from storage vessels in space may occur under various conditions. To analyze the influence of different leakage positions on the diffusion of tritium gas, simulations were carried out for tritium leakage below the air inlet, away from the vents, and below the air outlet. The tritium flow velocity fields in the leakage orifice plane and air outlet plane were attained at different times under the three leakage conditions, as shown in Fig. 5a–e. Five monitoring points were selected to monitor the variation in tritium concentration at different positions, and the variation law of tritium concentration with respect to time at the monitoring points under the three leakage conditions was obtained, as depicted in Fig. 6.

Figure 5a, b shows the tritium flow velocity field distribution in the leakage orifice plane and air outlet plane below the air inlet. The results show that the direction of the tritium leakage velocity was opposite to the air inlet direction when the storage vessel was located below the air inlet. At the initial leakage stage ($t=3$ s), a counterclockwise vortex was formed on the left side of the leakage orifice plane. When the leakage stopped ($t=5$ s), complex vortices were formed near the air inlet. After the air flow stabilized ($t=10$ s), two vortices in opposite directions were formed on the right side of the leakage orifice plane, as displayed in Fig. 5a. Moreover, a strong counterclockwise vortex was

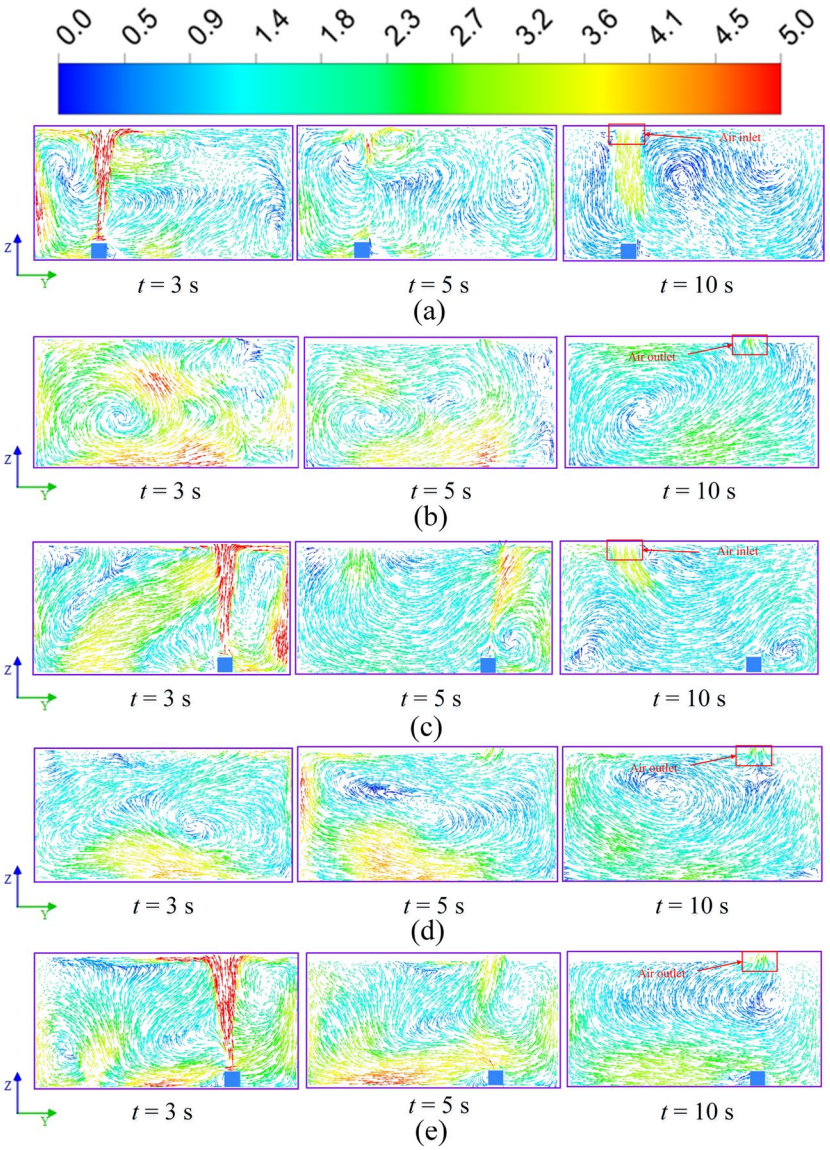

Fig. 5 (Color online) Velocity vector of tritium. **a** Velocity vector below the air inlet at $x=2.25$ m in the *YZ* plane; **b** velocity vector below the air inlet at $x=0.75$ m in the *YZ* plane; **c** velocity vector away from the vents at $x=2.25$ m in the *YZ* plane; **d** velocity vector away from the vents at $x=0.75$ m in *YZ* plane; **e** Velocity vector below the air outlet at $x=0.75$ m in the *YZ* plane

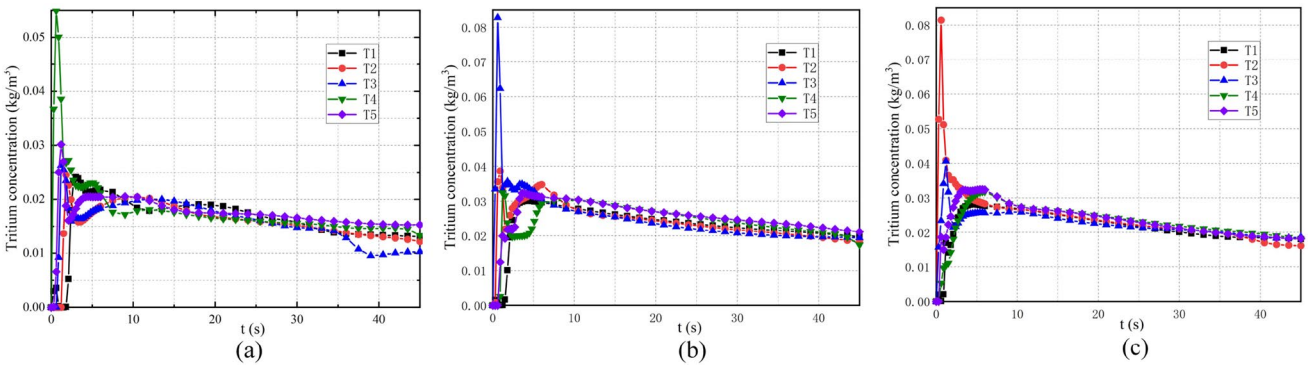

Fig. 6 (Color online) Variations of tritium concentration at each monitoring point in different leakage positions. **a** Below air inlet; **b** away from the vent; **c** below air outlet

formed on the left side of the air outlet plane, and the air in the plane mainly flowed to the vent outlet after gradual stabilization, as shown in Fig. 5b. Figure 5c, d shows the tritium flow velocity field distribution in the leakage orifice plane and air outlet plane away from the vents. The results reveal that a large clockwise vortex was formed on the right side of the leakage orifice plane at the initial leakage stage ($t = 3$ s). After the leakage ended, the right vortex in the plane became smaller, and two small vortexes were formed at the left and right corners of the plane, respectively, as shown in Fig. 5c. In addition, a large clockwise vortex was formed in the middle of the air outlet plane, and after the air in the space stabilized, most of the air flowed away from the outlet, with only a small part flowing toward the outlet, as shown in Fig. 5d. Figure 5e shows the tritium flow velocity field distribution in the leakage orifice plane below the air outlet. The results show that at the initial leakage stage ($t = 3$ s), a clockwise vortex was formed on the right side of the plane, making the tritium leakage direction deviate away from the axis. After the leakage ended, the air in the upper area of the plane flowed toward the vent outlet, whereas that in the lower area flowed away from the outlet. In summary, the flow velocity field distribution below the air inlet in the space was complex, with the air mainly flowing toward the outlet area. The air in the upper area flowed to the air outlet in the case of leakage below the air outlet, whereas only a very small part of the air flowed toward the outlet in the case of leakage away from the vents.

Figure 6 shows the variation in tritium concentration at each monitoring point in space under the three leakage conditions. The results demonstrate that during the tritium leakage ($0 < t < 5$ s), the tritium concentration at each monitoring point fluctuated significantly under the three leakage conditions. In the case of leakage below the air inlet, the tritium concentration at P4, which was closest to the leakage position, showed a wider fluctuation range. In the case of leakage away from the vent, the tritium concentration at P3, closest to the leakage position, experienced a wider fluctuation range. Meanwhile, in the case of leakage below the air outlet, the tritium concentration at P2, closest to the leakage position, had a wider fluctuation range. After 10 s of tritium leakage, the tritium concentration at each monitoring point gradually stabilized under the three leakage conditions. The stabilized tritium concentration below the air inlet was markedly lower than that under the other two leakage conditions, indicating that the complex flow velocity field distribution below the air inlet caused the tritium in the space to dilute faster.

4.4 Obstacles in the scene space

When tritium leaks from storage vessels, there may be obstacles in the space that exert a certain impact on the migration of tritium gas. To analyze the influence of obstacles on tritium diffusion, an operator and a rectangular obstacle were placed in the space, and the simulation was performed 20 s after tritium leakage. The resulting cloud diagrams of tritium flow velocity in different planes are shown in Fig. 7a, and the variation in tritium concentration at each monitoring point in the space with time is shown in Fig. 7b.

Figure 7a shows the cloud diagrams of the tritium flow velocity in different planes after 20 s of tritium leakage. As indicated in the figure, the flow velocity in the plane near the operator and the rectangular obstacle was small, whereas that near the air inlet and in the margin area was large, confirming the influence of obstacles on the migration of tritium gas. Figure 7b displays the variation of tritium concentration at each monitoring point. Compared with the results in Fig. 6, the tritium concentration at each monitoring point still fluctuated from $t = 10$ s to $t = 25$ s with the presence of obstacles, indicating that the obstacles would disturb the flow of gas and increase the time for the tritium concentration to reach stabilization.

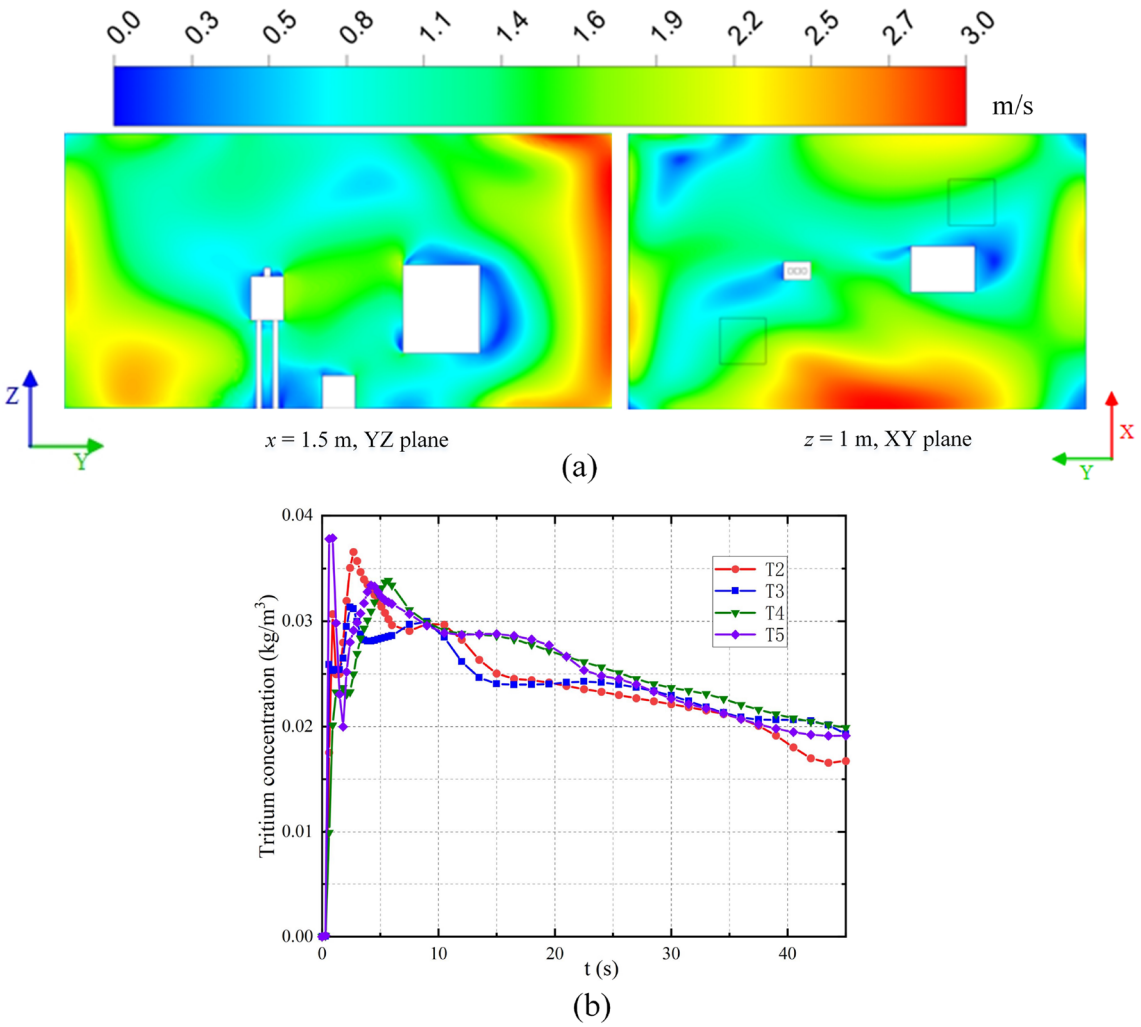

Fig. 7 (Color online) Simulation results of obstacle condition. **a** Cloud diagrams of tritium flow velocity in different planes at $t = 20$ s; **b** variations in tritium concentration at monitoring points with obstacles in space

5 Conclusion

In this study, the factors influencing tritium leakage and diffusion in indoor high-pressure storage vessels were investigated through a numerical simulation of tritium leakage based on FLUENT software. Specifically, the effects of the leakage orifice shape, leakage position, and presence of obstacles on tritium leakage and diffusion were analyzed. The findings are summarized as follows. First, when tritium leaks from the storage vessels, the symmetrical leakage orifice exerts less influence on the radial diffusion of tritium gas. The long axis of the rectangular leakage orifice is conducive to the radial diffusion of tritium gas, whereas the short axis inhibits the radial diffusion of tritium gas, and the axis conversion phenomenon becomes more prominent with a larger rectangle aspect ratio. Second, when tritium leaks from the storage vessels below the air inlet, the tritium in the scene space is diluted rapidly. However, when leakage occurs away from the air vents, the tritium concentration decreases slowly. Finally, obstacles in the scene space hinder the migration of tritium gas and increase the time for the tritium concentration to reach stabilization. This study provides a theoretical basis for tritium disposal in extreme tritium leakage accidents by analyzing the influence of different leakage conditions on the diffusion of tritium gas.

Author contributions All authors contributed to the study conception and design. Material preparation, data collection and analysis were performed by Chang-Jun Li, Xing-Fu Cai, Ming-Qing Xiao, Yong-Gang Huo, Peng Xu, Su-Fen Li and Xiao-Yan Cao. The first draft of the manuscript was written by Chang-Jun Li and all authors commented on previous versions of the manuscript. All authors read and approved the final manuscript.

References

1. M. Feng, Y.J. Wei, D.H. Li et al., Establishment of tritium activity concentration standard device. Radiat. Prot. **40**, 271–277 (2020). (**in Chinese**)
2. F. Zhao, S.-L. Zou, S.-L. Xu et al., A novel approach for radionuclide diffusion in the enclosed environment of a marine nuclear reactor during a severe accident. Nucl. Sci. Tech. **33**(2), 19 (2022). https://doi.org/10.1007/s41365-022-01007-z
3. M. Esfandiari, G. Jahanfarnia, K. Sepanloo et al., Loss of Offsite Power (LOOP) accident analysis by integration of deterministic and probabilistic approaches in Bushehr-1 VVER-1000/V446 Nuclear Power Plant. Nucl. Sci. Tech. **33**(5), 56 (2022). https://doi.org/10.1007/s41365-022-01044-8
4. K. Deng, L. Wang, Z.-H. Xia et al., Tritium concentrations in precipitation in Shanghai. Nucl. Sci. Tech. **29**(5), 63 (2018). https://doi.org/10.1007/s41365-018-0412-2
5. B.-E. Wang, S.-C. Zhang, Z. Wang et al., Numerical analysis of supersonic jet flow and dust transport induced by air ingress in a fusion reactor. Nul. Sci. Tech. **32**(7), 73 (2021). https://doi.org/10.1007/s41365-021-00912-z
6. M. Barzegari, M. Aghaie, A. Zolfaghari, Assessment of fuel-rod meltdown in a severe accident at Bushehr nuclear power plant (BNPP). Nul. Sci. Tech. **30**(4), 55 (2019). https://doi.org/10.1007/s41365-019-0589-z
7. Z.-X. Gu, Q.-X. Zhang, Y. Gu et al., Verification of a self-developed CFD-based multi-physics coupled code MPC-LBE for LBE-cooled reactor. Nul. Sci. Tech. **32**(5), 52 (2021). https://doi.org/10.1007/s41365-021-00887-x
8. R.V. Carlson, F.A. Damiano, K.E. Binning, Operation of the room air tritium removal system at the Tritium Systems Test Assembly. Fusion Technol. **8**, 2190–2195 (1985). https://doi.org/10.1016/0020-708X(85)90140-1
9. T. Hayashi, K. Kobayashi, Y. Iwai et al., Tritium behavior intentionally released in the radiological controlled room under the US-Japan collaboration at TSTA/LANL. Fusion Technol. **34**, 521–525 (1998). https://doi.org/10.13182/FST98-A11963665
10. K. Kobayashi, T. Hayashi, Y. Iwai et al., Tritium behavior intentionally released in the room. Fusion Sci. Technol. **54**(1), 311–314 (2008). https://doi.org/10.13182/FST08-A1820
11. Y. Iwai, T. Hayashi, T. Yamanishi et al., Simulation of tritium behavior after intended tritium release in ventilated room. J. Nucl. Sci. Technol. **38**(1), 63–75 (2001). https://doi.org/10.1080/18811248.2001.9715008
12. T. Hayashi, K. Kobayashi, Y. Iwai et al., Tritium behavior in the Caisson, a simulated fusion reactor room. Fusion Eng. Des. **51–52**, 543–548 (2000). https://doi.org/10.1016/S0920-3796(00)00214-3
13. Y. Iwai, T. Hayashi, K. Kobayashi et al., Simulation study of intentional tritium release experiments in the caisson assembly for tritium safety at the TPL/JAERI. Fusion Eng. Des. **54**, 523–535 (2001). https://doi.org/10.1016/S0920-3796(00)00581-0
14. K. Munakata, T. Wajima, K. Hara et al., Tritium release experiments with CATS and numerical simulation. Fusion Eng. Des. **85**, 1250–1254 (2010). https://doi.org/10.1016/j.fusengdes.2010.03.011
15. I.R. Cristescu, J. Travis, Y. Iwai et al., Simulation of tritium spreading in controlled areas after a tritium release. Fusion Sci. Technol. **48**(1), 464–467 (2005). https://doi.org/10.13182/FST05-A966
16. W. Li, H. Kou, X. Zeng et al., Numerical simulations on the leakage and diffusion of tritium. Fusion Eng. Des. **159**, 111749 (2020). https://doi.org/10.1016/j.fusengdes.2020.111749
17. G.Y. Liu, Simulation study of accidental tritium release on tritium extraction system of TBM. Thesis M. A. University of South China (2017) **(in Chinese)**
18. S.P. Wei, Study on inner fuel cycle and tritium transport simulation for CFETR tritium plant. Thesis M. A. University of Science and Technology of China (2021) **(in Chinese)**
19. C. Li, X. Cai, M. Xiao et al., Analysis on emergency treatment effect of tritium leakage accident in the nuclear reactor under different ventilation conditions. Front. Energy Res. **10**, 963990 (2022). https://doi.org/10.3389/fenrg.2022.963990
20. X. Cai, C. Li, Y. Huo et al., Study on emergency ventilation optimization method for tritium leakage accident of high-pressure storage vessel. AIP Adv. **12**(6), 065302 (2022). https://doi.org/10.1063/5.0096435
21. X.F. Li, J.L. Bi, M.C. David, Thermodynamic models of leaks from high-pressure hydrogen storage systems. J. Tsinghua Univ. (Sci.&Tech.) **53**(4), 503–508 (2013). https://doi.org/10.16511/j.cnki.qhdxxb.2013.04.027
22. I.A. Johnston, The noble-abel equation of state: thermodynamic derivations for ballistics modelling. Defence Science and Technology Organisation Edinburgh (Australia) Weapons Systems Div (2005)
23. T.H. Shih, W.W. Liou, A. Shabbir et al., A new k–ϵ eddy viscosity model for high reynolds number turbulent flows. Comput. Fluids **24**(3), 227–238 (1995). https://doi.org/10.1016/0045-7930(94)00032-T
24. J.B. Huang, *Industrial Gas Manual* (Chemical Industry Press, Beijing, 2002). (**in Chinese**)